MASSACHUSETTS INSTITUTE OF TECHNOLOGY
ARTIFICIAL INTELLIGENCE LABORATORY

A.I. Memo No. 1618 December, 1997

A Perturbation Scheme for Spherical Arrangements with Application to Molecular Modeling *

Dan Halperin †
Tel Aviv University

Christian R. Shelton ‡
Massachusetts Institute of Technology

Abstract: We describe a software package for computing and manipulating the subdivision of a sphere by a collection of (not necessarily great) circles and for computing the boundary surface of the union of spheres. We present problems that arise in the implementation of the software and the solutions that we have found for them. At the core of the paper is a novel perturbation scheme to overcome degeneracies and precision problems in computing spherical arrangements while using floating point arithmetic. The scheme is relatively simple, it balances between the efficiency of computation and the magnitude of the perturbation, and it performs well in practice. In one O(n) time pass through the data, it perturbs the inputs necessary to insure no potential degeneracies and then passes the perturbed inputs on to the geometric algorithm. We report and discuss experimental results. Our package is a major component in a larger package aimed to support geometric queries on molecular models; it is currently employed by chemists working in 'rational drug design.' The spherical subdivisions are used to construct a geometric model of a molecule where each sphere represents an atom. We also give an overview of the molecular modeling package and detail additional features and implementation issues.

---

*This work has been supported in part by a grant from Pfizer Central Research. Dan Halperin has also been supported in part by an Alon Fellowship, by ESPRIT IV LTR Project No. 21957 (CGAL), by the USA-Israel Binational Science Foundation, by The Israel Science Foundation founded by the Israel Academy of Sciences and Humanities, and by the Hermann Minkowski – Minerva Center for Geometry at Tel Aviv University. This document can be retrieved by anonymous ftp to publications.ai.mit.edu.

†Department of Computer Science, Tel Aviv University, Tel Aviv 69978, Israel. E-mail: `halperin@math.tau.ac.il`.

‡Department of Computer Science, MIT, Cambridge, MA 02139. E-mail: `cshelton@ai.mit.edu`. Part of the work on this paper was carried out while Christian Shelton was at the Department of Computer Science, Stanford University

1 Introduction

1.1 Background

Implementing geometric algorithms can be a difficult task. It has been found out and repeatedly rediscovered that there is a huge gap between geometric algorithms as they are described in most theoretical papers and their implementation in software. Two issues that are often ignored in the theoretical approach turn out to be critical in practice: Degeneracies and numerical precision. These issues are collectively referred to as "robustness" and they have been the topic of extensive research. Surveys on the topic can be found in [24],[27],[36], also several brief state-of-the-art summaries on the topic are collected in [25].

In theory degeneracies are often handled by assuming *general position*, namely assuming that degeneracies do not occur. The general position assumption had contributed significantly to the advancement of geometric algorithms by letting the researchers focus on the key (theoretical) problems while ignoring many technical issues. When implementing a geometric algorithm however, degeneracies must be taken into consideration.

The numerical precision problem was solved in the theory of geometric algorithms by assuming infinite precision real arithmetic [28]. For certain algorithms and geometric objects this assumption is realizable in practice by using *exact arithmetic* [1],[3],[4],[6],[15],[31],[37]. Computing with exact arithmetic is in general more costly than using floating point arithmetic, and in certain cases not realizable because of the geometric primitives that need to be manipulated. Here again there is a gap between what could in theory be handled by exact arithmetic and what current technology offers [14].

The software package that we describe in this paper computes the boundary of a union of spheres, the surface area of the boundary, and the intersection pattern of any sphere with all the other spheres in a given set. We therefore have to compute the intersection of pairs and triples of spheres, various tangency points of great circles and *little circles*[1] on a sphere, and so on. Such computations are not straightforward to carry out using exact arithmetic (all these operations require the solution of polynomial equations, so theoretically symbolic schemes could possibly be used here). Also floating point arithmetic has the obvious advantages of availability and efficiency. Our goal here is to devise robust algorithms that deal with intersecting spheres in $\mathbb{R}^3$ while using floating point arithmetic. Some examples of previous and related work on robust floating point geometric algorithms can be found in [17],[18],[22],[27],[32], and [33].

Our motivating application is geometric modeling of molecules. Our software package is part of a toolbox aimed to support the chemist in the drug design process [12],[13]. The basic geometric model of a molecule that we use is the so-called *hard sphere model* where every atom is represented by a sphere at some fixed position relative to the other atom spheres in the molecule. Since the hard sphere model is an approximate model to begin with, we have the freedom to perturb the spheres slightly without much effect on the relevance of the model.

When computing with floating point arithmetic we cannot precisely determine degeneracies; we can only know that we are in a potentially degenerate situation. For example, we may not be able to determine for sure that four spheres in our collection meet at a single point, but we could detect that the point of intersection of three out of the four spheres is less than some $\varepsilon > 0$ away from a point of intersection of a different triple of these spheres. For a small parameter $\varepsilon > 0$ which we call the *resolution parameter*, we regard such a pair of intersection points as a *degeneracy*. (A "potential degeneracy" may be a more appropriate term, but for brevity we will refer to such a situation as degeneracy.) Our new scheme guarantees that for a given parameter $\varepsilon > 0$, all the features of the spherical arrangement are at least ε apart (a formal definition of the ε-separation is given in

[1] Throughout the paper we use the term *little circle* to mean any circle on a sphere S that is the intersection of S with another sphere.

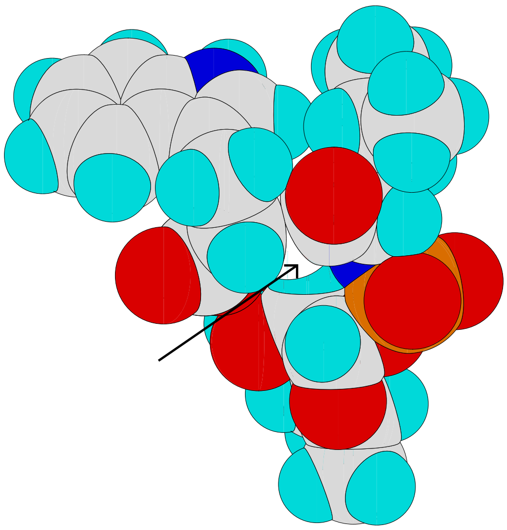

Figure 1: The sphere model of a molecule. The arrow points to the sphere whose spherical arrangement is drawn in Figure 2 (a).

Section 4). The resolution parameter ε depends on the floating point precision and on the type of operations (e.g., computing the intersection points of three spheres). We assume here that ε is given. There are numerical analysis methods to compute useful bounds on ε; see [23, Chapter 4] for examples concerning linear objects. We point out that in our algorithms the 'depth of operations', namely how many times in a row the result of one operation is the operand in another operation, is bounded by a small constant. Therefore one can obtain a bound on the resolution parameter that does not depend on the input size n—the number of spheres, in our case.

1.2 Summary of Results

We present an efficient perturbation scheme for a collection M of n spheres in $\mathbb{R}^3$ that makes our geometric algorithms robust. We call the decomposition of $\mathbb{R}^3$ induced by the spheres the *arrangement of the spheres*; the subdivision of each sphere by the circles of intersection with other spheres we call a *spherical arrangement*. We denote the maximum number of spheres in M intersecting any single sphere in M by k (as was shown in [21], k is a constant for the hard sphere model of molecules; see also Section 2.2). For any given resolution value $\varepsilon > 0$, we determine a parameter δ that depends on ε, on k, and on the maximum radius R of a sphere in M. We then present a scheme that perturbs each sphere by at most δ, resolves all the degeneracies in the arrangement of the spheres, and runs in $O(n)$ time.

We also take care of degeneracies that result from a further decomposition (or refinement) of the spherical arrangements known as the *trapezoidal decomposition* (see Section 2.1). Since in the trapezoidal decomposition we are free to choose a direction for the 'poles' (two antipodal points on a sphere, such that all the arcs added in the refinement are portions of great circles through these poles), we choose the poles so that the angular separation of the added arcs will be above a certain threshold ω. Here also, we choose ω such that determining the poles could be done fast.

We have implemented this perturbation scheme and we report experimental results below. For example, letting $\varepsilon = 10^{-11}$, $\delta = 10^{-9}$, and $\omega = \arccos(1 - 10^{-11})$, loading a molecule with 2034 atoms (namely computing the boundary surface and all the individual spherical arrangements) takes 146.8 seconds, including the perturbation time, on an SGI Indigo 250Mhz RS4400. Our experimental results show that in most cases the time taken up by the perturbation scheme is negligible (Section 6).

Our software is part of a toolbox of data structures and algorithms aimed to support the chemist in the *rational drug design* process [2], and it is currently being used by chemists in a pharmaceutical company. Further details on the larger software (the toolbox) can be found in [12].

1.3 Comparison with Related Work

As mentioned above our approach to robustness can be categorized as fixed precision approximation. The approximation is achieved by a controlled perturbation that removes all degeneracies. Our approach requires a detailed analysis of all degenerate cases that can arise in the arrangement and its refinement. In that sense it shares a feature with the work of Burnikel et al.[5] that solicits the direct handling of degeneracies. Of course the big difference between our approach and theirs is that they use exact arithmetic. To explain the advantages and disadvantages of both approaches, let's take a look at what most algorithms that compute arrangements do.

A typical algorithm for computing arrangements consists of two intertwined parts: (i) computing features, usually vertices of the arrangements and special points such as points of vertical tangency, and (ii) computing adjacencies between features to create a 'map' of the subdivision that can be traversed, cell by adjacent cell. The first step is usually ignored in the computational geometry literature (unless some sophisticated data structures are necessary to identify the features) and when it is non-trivial, the difficulty lies in the algebra. The second step is more challenging, especially when degeneracies need to be taken into account. Burnikel et al. [5] handle degeneracies also at the second stage. Indeed they achieve a clean solution for a 2D problem. We work with degeneracies only at the first stage, which is much simpler since we only work with features rather than with adjacencies. When our algorithm gets to the second stage it is guaranteed that all degeneracies have been removed and this makes programming far simpler. We believe that extending their approach to three and higher dimensions will be a difficult task, because of the large number of special cases that needs to be handled; this has motivated the body of research on perturbations schemes for a long time [10],[11],[30],[35]. It would be interesting to compare the methods for three-dimensional arrangements—the setting of our work.

The obvious disadvantage of our approach relative to theirs and to any scheme that uses exact arithmetic is that we approximate the input, which may be unacceptable in certain applications. However, for many applications a slight approximation is permissible. A large number of engineering and physical world models are approximate to start with, and a controlled perturbation of the type proposed here is within the error bounds of the measurement/model. Moreover, there are application domains where workers prefer approximations of geometric objects to precise objects, because running time, for example, is more important than precision. In such cases, our scheme, if applied, can be viewed as part of the approximation.

Another approach in the framework of fixed precision approximation is *snap rounding* [22]. This approach has been recently revisited [17] and has been successfully implemented for two-dimensional arrangements of segments. The disadvantage of this approach relative to ours is that not only snap-rounding does not resolve degeneracies, it in fact creates degeneracies. In two-dimensional arrangements this hardly has any effect on the difficulty of programming, but we believe that in three-dimensional space (e.g., arrangements of triangles in 3-space), again because of the variety of degenerate cases, it would be much more difficult to define and implement.

A common approach to fixed precision robustness, in the folklore of practitioners of geometric computing, is as follows: apply a small random perturbation to all the input objects, then run the algorithm, and if a problem[2] occurs, start again by applying a random perturbation to the objects. Our scheme is different in several ways. Our scheme is guaranteed to succeed (provided that the right parameters are chosen) and it is guaranteed to work efficiently. The efficiency comes in part from the fact that we work incrementally, and once we have finished inserting an object to the arrangement (possibly after several attempts of inserting it in different places) we will not move this object again. The price that we pay is in the detailed analysis of degeneracies, and programming the tests to check if they arise.

If degeneracies are not removed, either exact arithmetic must be used to determine precisely when an exact degeneracy occurs and the geometric algorithm must take such cases into account, or the algorithm will fail. The nature of the failure depends on the algorithm. In the case considered here, during the construction of the surface patches the connectivity of the patches will be self conflicting (i.e., the graph of patch connectivity will no longer correspond to a valid topology). This results either in the algorithm entering an infinite loop (since the assumptions on which it was based have been violated) or in surface area calculations which make no physical sense (e.g., some spheres are attributed with negative surface areas or with a contribution to the surface greater than the total surface area of the sphere).

Ours is definitely not the first implementation of an algorithm for computing molecular surfaces; see, e.g., [7],[9],[29],[34] and the recent survey by Connolly [8]. We believe that our approach stands out in its efficient treatment of robustness issues, and in the ease and flexibility of computing substructures of the collection of the spheres, such as the union of a subset of the spheres of one molecule consumed by another molecule.

1.4 Paper Outline

The rest of the paper is organized as follows. In the next section we give more background details on spherical arrangements and on the hard sphere model of a molecule. In Section 3 we review our software package. The key ideas underlying our new perturbation scheme are presented in Section 4. Algorithmic details of the scheme and running time analysis are given in Section 5. In Section 6 we report experimental results. More practical issues concerning our implementation are discussed in Section 7. A brief summary and suggestions for future research on the topic are given in Section 8. In the Appendix we complete technical details concerning shapes and volumes that arise in the perturbation scheme.

2 Preliminaries: Spheres and Molecules

2.1 Little Circles on a Sphere

A collection of circles on a sphere S induces a partitioning of the sphere into vertices, edges and faces. We call such a partitioning a *spherical arrangement*; see Figure 2(a). If all the circles are great circles, then one can transform the spherical arrangement into a *planar arrangement of lines* [20], which is a simpler object to handle [16]. However, in our application the circles are not necessarily great circles. Each of the circles is the result of the intersection of S with another sphere. We refer to these more general circles as *little circles*.

The faces in the spherical arrangement need not be simply connected, and each face may have a large number of edges on its boundary. We can apply a standard refinement procedure, called a *trapezoidal decomposition* that will make each face homeomorphic to a disc and have at most four edges on its boundary, as illustrated in Figure 2(b); see, e.g., [20, Section 21.3] for more details on trapezoidal decompositions. In this context, we fix a pair of antipodal points as *poles*. We call the

[2] What *a problem* is depends on the algorithm and the implementation and refers to any unexpected or undesired outcome of the program.

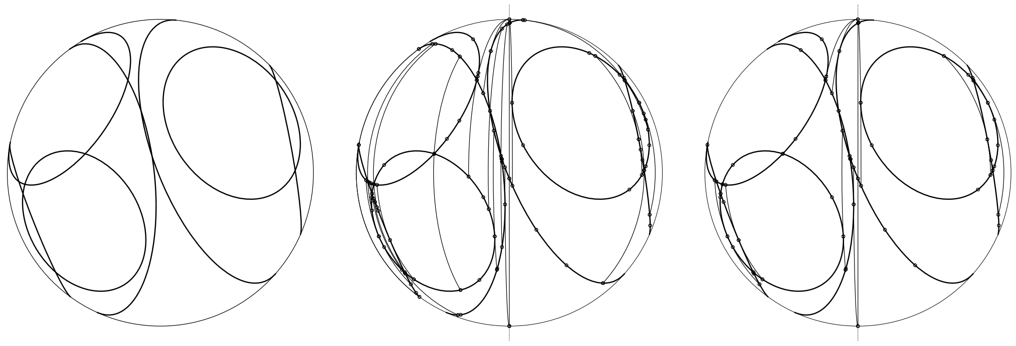

(a) (b) (c)

Figure 2: A spherical arrangement (a), its full trapezoidal decomposition (b), and partial trapezoidal decomposition (c).

great circles through the poles *polar circles*, arcs of polar circles *polar arcs*, and any point on a little circle that is tangent to a polar circle we call a *polar tangency*. For every polar tangency of every circle in our collection, we extend a polar arc in either direction until it hits another little circle or reaches a pole. We do the same from every intersection point of a pair of little circles. We call this refinement the *full trapezoidal decomposition*.

If we are only concerned with making each face simply connected and making the graph of all the edges of the arrangement connected then using a *partial trapezoidal decomposition*, in which polar arcs are only extended from polar tangency points and not from intersections, suffices. See Figure 2(c).

2.2 The Hard Sphere Model

A common approach to representing the three-dimensional geometric structure of a molecule is to represent each of its atoms by a "hard" sphere. In certain applications it is also assumed that the relative displacement of the spheres is fixed. There are recommended values for the radius of each atom sphere and for the distance between the centers of every pair of spheres. In this model, the spheres are allowed to interpenetrate one another, therefore it is sometimes referred to as the "fused spheres" model (see Figure 1). The envelope surface of the fused spheres may be regarded as a formal *molecular surface*. It is evident that various properties of molecules are disregarded in this simple model. However, in spite of its approximate nature, it has proven useful in many practical applications. For more background material and references, see for example the survey paper by Mezey [26].

In [21] the hard sphere model is studied from a *computational geometry* point of view. Several observations are made in that paper showing that, because of certain special properties, the spheres in this model can be efficiently manipulated. We cite below the results that will be needed in later sections. Theorem 2.1 states the conditions that make the sphere model of a molecule favorable. Theorem 2.2 summarizes a hash-table based data structure that is constructed exploiting these conditions.

Theorem 2.1 [21] *Let $M = \{B_1, \ldots, B_n\}$ be a collection of n balls in 3-space with radii $r_1, \ldots, r_n$ and centers at $c_1, \ldots, c_n$. Let $r = \min_i r_i$ and let $R = \max_i r_i$. Also let $S = \{S_1, \ldots, S_n\}$ be the collection of spheres such that S_i is the boundary surface of B_i. If there are positive constants ρ_1, ρ_2 such that $\frac{R}{r} < \rho_1$ and for each B_i the ball with radius $\rho_2 \cdot r_i$ and concentric with B_i does not contain*

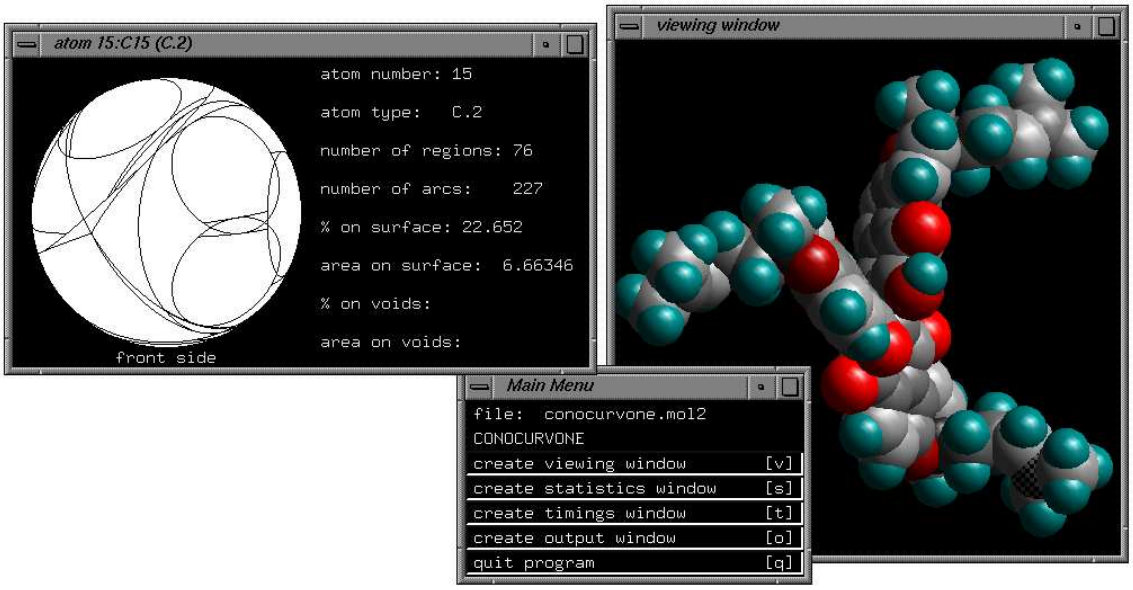

Figure 3: Screen shot of interactive application showing the molecule conocurvone. A carbon atom, the checked one on the lower right of the viewing window, has been selected and the partial vertical decomposition for it is shown in the upper left window. The viewing window displays the molecule with each atom colored by element type and shaded by area contributed to the surface.

the center of any other ball in M (besides c_i), then: **(i)** *for each $B_i \in M$, the maximum number of balls in M that intersect it is bounded by a constant, and* **(ii)** *the maximum combinatorial complexity of the boundary of the union of the balls in M is $O(n)$.*

Theorem 2.2 [21] *Given a collection M of n balls as defined in Theorem 2.1, one can construct a data structure using $O(n)$ space, to answer intersection queries for balls whose radii are not greater than R, the maximum radius of the balls of M, in $O(1)$ time. The expected preprocessing time of the structure is $O(n)$.*

3 Overview of the Software Package

The algorithms described in the paper are embedded in a couple of different applications for computational chemists. One of these applications is a batch processor to take a single molecule or pairs of molecules and compute and output surface statistics. The other application is a real-time viewer with which the user can manipulate a three-dimensional model of the molecule (or pair of molecules) and display various statistics through either the shading and color of the model at different atoms, or through other three-dimensional models of individual atoms. A screen shot of this second application can be seen in Figure 3.

Among the surface calculations interesting to chemists are the surface area, the void areas (the area of the boundry of hidden "void pockets" in the molecule or between two molecules), and the interaction of surface areas. All of these statistics are useful on a per atom basis. The last statistic (surface interaction) is of special interest. For this, the user would like a measure of what portion of one molecule is "eaten" by (or part of the intersection of) another. A measure of the intersection of the two molecules, broken down by atom, helps the user to understand which atoms of the drug and protein are involved in the binding of the drug molecule. It is important to understand which features of the drug molecule are necessary and which are changeable during the course of novel drug design.

There are many different measures of such a consumption. For our program, we chose to report the difference of the surface area of the two molecules together (and intersecting) and the area of the molecules separately. Since we explicitly decompose each sphere by all the little circles of intersection, we can be very flexible in our surface computations.

In order to construct the surface, a seed patch (or a surface region guaranteed to be on the surface) is found and the surface is grown by following the connectivity of the spherical decompositions. In our search, when crossing an edge created by a little circle, we have the choice of continuing on the current sphere or jumping to the intersecting sphere. To construct the entire surface, we always choose to change spheres. However, we can remove any arbitrary set of spheres from an already constructed decomposition simply by choosing to stay on the current sphere when crossing any edge made by an intersection with a sphere in the omitted set.

In this manner, the decomposition of spheres can be computed once and then reused for any surface calculation needed including: omitting certain atoms (like all hydrogens), considering only certain types of atoms, or omitting whole molecules. In addition, surface calculations can attribute to each atom its portion of the surface area.

This paper will concentrate on the robust computation of the spherical decompositions. Higher level data structures for keeping track of atoms within multiple molecules and lower level code for computing intersections and storing the geometry of points and arc segments will be assumed for our discussion.

For representing the spherical decompositions, we chose a variant of the quad-edge data structure [19]. This structure makes updating the subdivision simple. Each arc is stored as a plane and two points (thus the arc is the intersection of the plane and the sphere between the two points). Four operations are needed: adding an arc, removing an arc, splitting an arc, and merging two connected arcs (namely two arcs that belong to and are adjacent along a single circle). The maintenance of this data structure is fairly standard and we omit the details here.

The data structure representing the spherical arrangement assumes that the graph of arcs is connected. This means that all of the regions must be simply connected. To ensure this, we break up the surface with additional arcs in order to create a trapezoidal decomposition, as described in Section 2.1.

We have presented so far the ingredients that are necessary to understanding the perturbation scheme. Further details on our software implementation are given below in Section 7.

4 The Perturbation Scheme

We distinguish two types of degeneracies that arise in a collection M of intersecting spheres and atom maps as we compute them. Recall that we are concerned with floating point arithmetic and that we define a degeneracy using a resolution parameter $\varepsilon > 0$. In this section we give a precise definition of the various degeneracies. We describe the two types as they occur on a single sphere. See Figure 4.

Type I A little circle is too small, two little circles are tangent (or almost tangent), or two intersection points each being the intersection of three spheres are close together. Had we been using exact arithmetic these (potential) degeneracies would correspond respectively to the following exact degeneracies in the three-dimensional arrangement of spheres: Two spheres are tangent to one another, three spheres intersect in a single point, or four spheres intersect in a point.

Type II The angle between the planes containing two distinct polar arcs is too small (it is below some threshold ω).

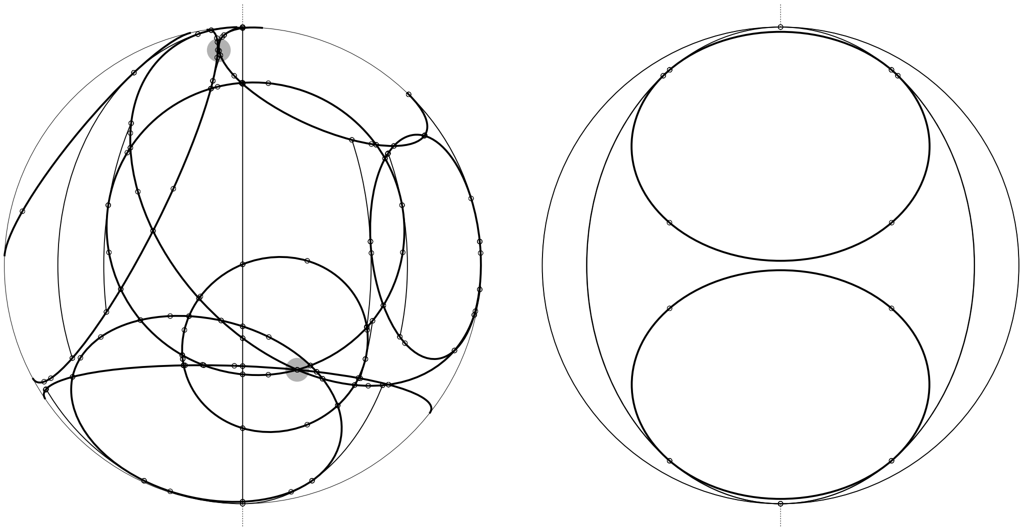

Figure 4: Examples of the two types of degeneracies. Type I degeneracies are marked by small shaded circles.

Type I is inherent to the arrangement of spheres, whereas type II is an artifact of our decomposition method.

We wish to perturb the spheres slightly so that all the features of the arrangement will be at least ε apart, for a given resolution parameter ε; an exact and formal definition of "features being ε-apart" is given in the following section. We would like the perturbation procedure to be efficient and at the same time that the perturbation magnitude will be as small as possible. For a given ε our procedure will determine a perturbation value δ that will guarantee that the procedure will take $O(n)$ time for n spheres.

We use a two-step perturbation scheme:

Step 1. We remove type I degeneracies by an incremental procedure where we add the spheres one-by-one and if a degeneracy occurs we only perturb the last sphere that has been added.

Step 2. We choose the orientation of the pole (namely the direction to which all of the planes containing polar arcs will be parallel) that will eliminate degeneracies of type II.

4.1 Removing Type I Degeneracies

Let $S_1, S_2, \ldots, S_n$ be an ordering of the spheres in M. For a pair of spheres S_i and S_j let ρ_{ij} denote the distance between their centers. Let M_t denote the set $\cup_{i=1}^{t}\{S_i\}$. After the completion of stage t, the incremental procedure will maintain the following invariants:

I_1 The center of any sphere in M has been moved by at most δ from its original placement (δ is a constant to be determined below).

I_2 For every pair of distinct spheres S_i and S_j, $i, j \leq t$, and $r_j \geq r_i$, we have $|\rho_{ij} - r_i - r_j| > \varepsilon$ and $|\rho_{ij} + r_i - r_j| > \varepsilon$.

I_3 For every triple of distinct spheres S_i, S_j and S_k, $i, j, k \leq t$, the circle $C_{ij} := S_i \cap S_j$ and the sphere S_k are not tangent, and are at least ε away from being tangent. (The formal definition of this invariant is given in the Appendix.)

I_4 Let τ_i and τ_j each be an intersection point of three spheres in M_t; then $d(\tau_i, \tau_j) > \varepsilon$.

Invariants I_2 through I_4 correspond to insuring that the degeneracies of type I are avoided by a margin of at least ε. We call a perturbation scheme that satisfies the above invariants at the end of each stage (and in particular after the nth stage) a *valid perturbation scheme*.

Suppose that the procedure has been carried out successfully for the first t stages. We next describe how we add the sphere S_{t+1} so that M_{t+1} will maintain the invariants above. We denote the center of sphere S_i for $i \leq t$ after the completion of step t by C'_i. Let $B(C_{t+1}, \delta)$ be the ball of radius δ around the original placement of the center C_{t+1} of S_{t+1}. We will place the center of S_{t+1} inside $B(C_{t+1}, \delta)$ and this will guarantee the invariant I_1. The invariants I_2, I_3 and I_4 define forbidden loci F_2, F_3 and F_4 respectively for the center of S_{t+1}. We will choose the new placement C'_{t+1} of the center of S_{t+1} to be in $G_{t+1} := B(C_{t+1}, \delta) \setminus (F_2 \cup F_3 \cup F_4)$. If such a placement exists, we call it a *valid placement* of the center of S_{t+1}. If the original placement of S_{t+1} lies in G_{t+1} then we do not move S_{t+1}—this will guarantee that if the features of the arrangement of the input spheres are already ε-apart, no perturbation will take place.

The region F_2 is the union of *spherical shells*[3] of two types. Each sphere $S_i \in M_t$ induces two spherical shells according to whether the tangency is external (namely, at the tangency point the interior of the spheres are disjoint) or internal. One shell has its center in C'_i and its radii are $r_i + r_t - \varepsilon$ and $r_i + r_t + \varepsilon$. This spherical shell represents the loci of placement of the center of S_t that result in the spheres S_i and S_t being tangent, or almost tangent. The other type of shells is defined similarly.

We postpone a detailed explanation of the shape of the objects contributing to F_2, F_3, and F_4 to the Appendix. We just mention that F_4 is also the union of spherical shells, whereas F_3 is the union of *toric shells*. In the Appendix we derive upper bounds on the volume taken up by the regions F_2, F_3, and F_4. Let $VF := \text{Volume}(F_2 \cup F_3 \cup F_4)$ and let $VB := \text{Volume}(B(C_{t+1}, \delta))$.

Our goal is to choose δ such that $VB > 2 \cdot VF$. If we do that, we are guaranteed that a point chosen uniformly at random inside $B(C_{t+1}, \delta)$ has probability $> \frac{1}{2}$ to be a valid placement for the center of S_{t+1}. Our calculations, which are given in the Appendix, show that we need to choose $\delta = f(k, \varepsilon, R) = 2k\varepsilon^{1/3}R^{2/3}$, where k is the maximum number of spheres in M intersecting any single sphere in M, R is the maximum radius of a sphere in M, and assuming $k \geq 10$. Not surprisingly, our experimental results show that this is a very conservative bound. The theoretical bound is a crude worst-case bound, and even as such it shows that our approach does not conceal any very large constant.

4.2 Removing Type II Degeneracies

After we have removed all type I degeneracies, we wish to choose a direction for the poles such that no type II degeneracy arises, when using the **partial** vertical decomposition. (The method can be extended to deal with full vertical decomposition, and we report below experimental results for the full decomposition as well.) We will handle each sphere separately, namely choose the direction for the poles independently for each sphere.

The situation here is significantly different from the situation with type I degeneracies: It is impossible to guarantee an ε-separation of the polar arcs. Polar arcs can get arbitrarily close to one another, and they can coincide in the poles. Therefore our goal is to obtain a good angular separation, which we call *ω-separation*, and is defined as follows: Once the direction of the poles has

[3] A spherical shell is the region enclosed between two concentric spheres.

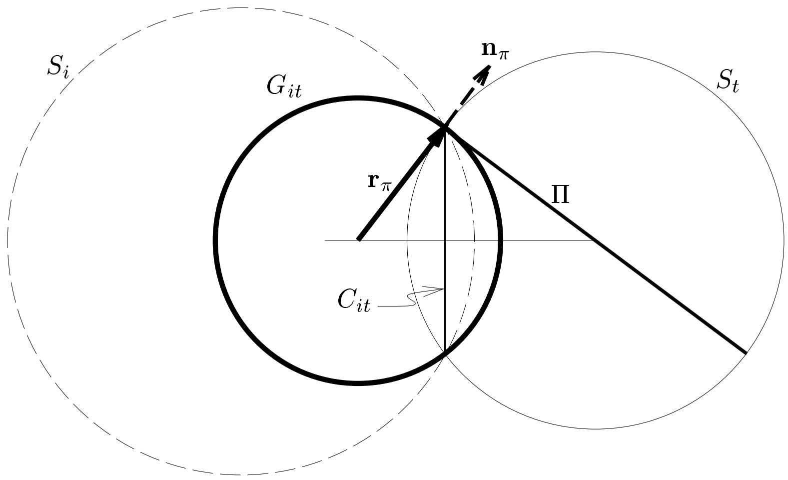

Figure 5: A cross-section of C_{it} and Π.

been determined, for any pair of distinct polar arcs the angle between the planes containing them is at least ω. We wish to determine the biggest ω that will allow us to run Step 2 efficiently. If ω-separation has been obtained for an ω value which is greater than the floating point resolution, polar arcs can be safely and consistently distinguished during computation.

We next describe this procedure for a single sphere S_t, after Step 1 has been completed (and type I degeneracies have been removed). Fix two little circles C_{it} and C_{jt} on S_t, each being the intersection of S_t with another sphere in M (S_i and S_j respectively), and let Φ be a great circle on S_t that is tangent to C_{it} and C_{jt}.

In general, Φ is one of at most four great circles tangent to these two little circles: There is a one-to-one mapping from great circles to planes passing through the center of the sphere (a great circle is the intersection of such a plane with the sphere). Let Π be a plane passing through the center of the sphere which we will parameterize by its normal $\mathbf{n}_\pi$ and, by an abuse of notation, we will also let $\mathbf{n}_\pi$ denote the point on the unit sphere such that the normal $\mathbf{n}_\pi$ is the difference of that point and the origin. If we restrict Π to pass tangent to the circle C_{it}, then $\mathbf{n}_\pi$ must lie on a little circle on the unit sphere.

This can be shown by constructing the sphere G_{it} whose center, g_{it}, lies on the lie between c_i and c_t such that for any point p on the circle C_{it}, $(\mathbf{p} - \mathbf{g}_{it})$ is parallel to $\mathbf{n}_\pi$ (see Figure 5). If we let $\mathbf{r}_\pi$ be the vector from g_{it} to p, we note that the set of all possible $\mathbf{r}_\pi$ forms a little circle (namely C_{it}) on the sphere G_{it}. Thus, since $\mathbf{n}_\pi$ is parallel to $\mathbf{r}_\pi$, we know that the normals to Π must lie on one of two little circles on the unit sphere (one corresponding to C_{it} and one corresponding to the reflection of C_{it} about g_{it} since if $\mathbf{n}$ is a normal of a plane, $-\mathbf{n}$ is also a normal of the same plane).

Thus, if we restrict Π to be tangent to two little circles (C_{it} and C_{jt}), we are restricting $\mathbf{n}_\pi$ to be at the intersection of two sets of two little circles on the unit sphere. This yields up to 8 solutions provided that the sets of little circles are not identical. However, since each solution will be produced along with its negative (which will correspond to the same plane and thus the same great circle), we conclude that unless C_{it} and C_{jt} are parallel and of the same radius, there will be at most four great circles of S_t which are tangent to both C_{it} and C_{jt}.

The circle Φ is the locus of pole locations that will cause the planes containing the polar arcs

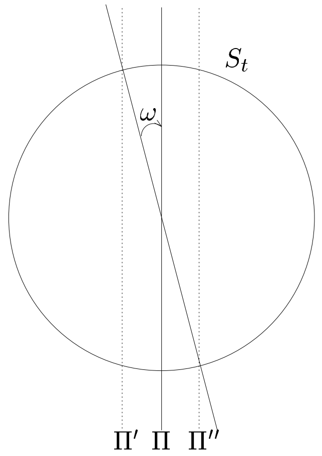

Figure 6: A cross-section of S_t.

extending from the tangency points of Φ with C_{it} and C_{jt} to coincide, namely have zero angular separation. For the moment, assume that there are only 4 possible positions for Φ. Let Π' and Π'' be two planes parallel to Π, each on a different side of Π, and such that any plane Π_0 passing through the center of S_t and tangent to the circle $\Pi' \cap S_t$ (or the circle $\Pi'' \cap S_t$) makes an angle ω with Π. See Figure 6 for an illustration. We call the portion of S_t between $\Pi' \cap S_t$ and $\Pi'' \cap S_t$ the ***ω-strip of** Φ*, and denote it by $\sigma(\omega, \Phi)$. It is easily verified that if the poles are chosen outside $\sigma(\omega, \Phi)$ then the polar arcs that correspond to the tangencies of Φ with C_{it} and C_{jt} are at least ω apart.

Every tangent circle Φ of every pair of circles on S_t defines an ω-strip $\sigma(\omega, \Phi)$. Assume without loss of generality that the radius of S_t is 1. The area of any such strip is $4\pi \sin \omega$. The maximum number of strips that need to be considered on S_t is $4\binom{k}{2}$. For Step 2 to run in $O(n)$ time we wish that at least half of the surface area of S_t will not be covered by ω-strips (any constant fraction will do; the smaller the uncovered fraction the higher the constant factor in the expected running time bound). Therefore we choose ω such that

$$2 \cdot 4\binom{k}{2} 4\pi \sin \omega < 2 \cdot 4\pi \implies \sin \omega < 1/(2k(k-1)) .$$

We now consider the case where C_{it} and C_{jt} are parallel and have equal radii, thus producing an infinite set of possible Φ. In this case, we are guaranteed that C_{it} and C_{jt} will lie on opposite sides of c_t (if they did not, it would violate the assumptions of Theorem 2.1). For any Φ, when we choose a pair of poles on Φ, we split Φ into two equal halves. In this degenerate case, for any choice of these poles, the two tangency points will be on different halves. Polar arcs can run, at maximum, from pole to pole (only one half of a great circle) and thus can be distinguished from polar arcs which run on the "other half" of the same great circle. Each tangency will induce at maximum a polar arc that will run on one half of Φ, but both will be on opposite sides of the poles thus can can be differentiated. Hence, we only need to be sure that the pole does not lie on or too close to the circles C_{it} or C_{jt} (which would cause another degeneracy). To do this, we add an additional constraint that the pole direction may not be within ϵ (the same ϵ as from the removal of type I degeneracies since we are attempting to distinguish between points) of any little circle.

Remarks.
(1) The ω-strip is only an inscribing region of the forbidden region corresponding to any Φ. The actual forbidden region induced by any tangency is in fact smaller, and it has a more complicated boundary.
(2) Extending the method to the full vertical decomposition requires handling several more cases involving up to four circles C_{it} each. This extension is straightforward and we omit further details here. We have implemented this extension and we report experimental results for it below.
(3) In practice, it is convenient to impose the same pole direction for all the spheres in the arrangement, for ease of coding, debugging and visualization. To this end we draw all the ω-strips on the unit sphere of pole directions $\mathcal{S}^2$, and the constraint on ω becomes $\sin\omega < 1/(4nk(k-1))$. The experimental results described below are for this choice of pole directions.
(4) The construction of the forbidden regions on S_t is diametrically symmetric, namely a point on S_t is free (i.e., represents a pole that will induce an ω-separation) if and only if its antipodal point is free.

5 Algorithmic Details and Complexity Analysis

In this section we describe how the perturbation scheme is carried out efficiently.

The incremental procedure of Step 1 will move the center of each sphere by at most δ from its original placement. We expand each of the original spheres S_t into a sphere S''_t whose radius is $r_t + \delta$, and let M'' be the set of the expanded spheres S''_t. We construct a data structure as described in Theorem 2.2 to support range queries on the spheres in M''. This structure enables us to find in $O(1)$ time all the spheres in M'' that intersect a given query sphere S''_t. Since we use expanded spheres, the structure can be used for detecting intersections with original as well as with perturbed spheres.

When looking for a perturbation of the center of S_t during Step 1 of the procedure we proceed as follows. Although constructing the subdivision of $B(C_t, \delta)$ into free and forbidden regions could be done in maximum constant time, it would be an extremely difficult task that may introduce new precision problems. Instead we do something much simpler. We choose a point p uniformly at random in the ball $B(C_t, \delta)$. We next check whether p is a valid perturbation by checking that it lies outside all the forbidden regions F_2, F_3 and F_4. For example, to check whether p lies outside F_2 we check whether it lies outside each of the at most $2k$ spherical shells defining F_2. Each of these tests is simple and fast and their overall number is bounded by a constant (see below for experimental results). Recall that δ was chosen such that with probability $> \frac{1}{2}$, the point p will represent a valid perturbation. Thus the expected number of trials before we find a valid p is ≤ 2, and the overall running time of Step 1 is $O(n)$.

Similar arguments apply to Step 2 procedure. For any given sphere S_t, we choose a point p uniformly at random on the boundary of $\mathcal{S}^2$. We then test all the ω-strips relevant to S_t to check whether p lies outside all those strips. By the choice of ω the expected number of trials before we find a valid p is ≤ 2, and the overall running time of Step 2 is $O(n)$ as well.

We summarize the performance of the perturbation scheme in the following theorem.

Theorem 5.1 *Given a collection M of n spheres as described in Theorem 2.1, and a resolution parameter $\varepsilon > 0$, a valid perturbation of the spheres in M can be computed in expected $O(n)$ time, by moving each sphere by at most δ from its original placement, where δ is a parameter that depends on ε, on the maximum number of spheres in M intersecting any single sphere in M, and on the maximum radius of a sphere in M, and such that all the degeneracies are resolved. In expected $O(n)$ time we can also find a direction for the poles on each sphere so that all the polar arcs in the trapezoidal decomposition of the spherical arrangements lie on planes the angle between any pair of*

number	file name	size	k	mean k'
1	estradiol.mol2	44	17	6.81
2	clofazimine.mol2	55	13	6.67
3	michellamine_b.mol2	104	13	6.81
4	288d.pdb	120	9	6.25
5	conocurvone.mol2	127	14	6.67
6	245d.pdb	240	9	6.17
7	1ppt.pdb	301	10	5.92
8	4pti.pdb	454	10	5.79
9	1bzm.pdb	2034	10	5.74
10	2pka.pdb	3598	11	5.79
11	2ace.pdb	4143	12	6.05
12	1sdk.pdb	4384	12	6.00
13	1nok.pdb	6759	11	5.73
14	7at1.pdb	7106	12	5.70

Table 1: Listing of the molecules used for testing. Molecules with file names ending in pdb can be found at the Protein Databank at http://www.pdb.bnl.gov/. Molecules with file names ending in mol2 can be found at the Center for Molecular Modeling at http://cmm.info.nih.gov/modeling/. The size column gives the number of atoms in the molecule, k' and k are explained in the beginning of Section 6

which is at least ω, for ω that depends on the maximum number of spheres in M intersecting any single sphere in M.

We emphasize again that the theoretical bounds that we obtain on δ and ω are crude and in practice (as shown next) these quantities are much smaller.

6 Experimental Results

In order to ease the explanation of the results, we introduce a new variable. Let k' be the number of spheres intersecting a given sphere in a given collection of spheres. Thus, k' is a function of a particular collection and a particular sphere and the constant k in the previous sections is then $\max k'$ over a collection of spheres. These values are listed in Table 1 for the fourteen molecules we chose for the timing experiments. The molecules from the Protein Databank did not specify the positions of hydrogen atoms whereas the others did. This accounts for most of the difference in k and k' values. All timings were done on an SGI Indigo with a 250Mhz MIPS RS4400 CPU.

For our timings, we ran the program on each of the molecules in our set for varying ϵ and δ: δ on $[10^{-6}, 10^{-10}]$ and ϵ on $[10^{-9}, 10^{-12}]$ to determine the experimental dependence of δ on ϵ. Figure 7 shows the results of these timings for the portion of the code not involved with computing perturbations. Figure 8 details the time spent in the perturbation code.

It should be noted that almost all of the perturbation time $(90 - 98\%)$ is spent finding the pole direction. Table 2 shows the fraction of the δ-spheres which are free, $(VB - VF)/VB$ in the notation of Section 4.1, and Table 3 shows the fraction of the pole directions that are free for a typical molecule. To obtain the former chart, we modified the program to attempt (and discard) 1000 perturbations each time the center of an atom was positioned. The values shown in the table are the average over all center placements of the fraction of these positions that were valid. The latter was obtained with a similar sampling method for pole directions.

The reason for the dramatic difference between the time spent on pole perturbation and the

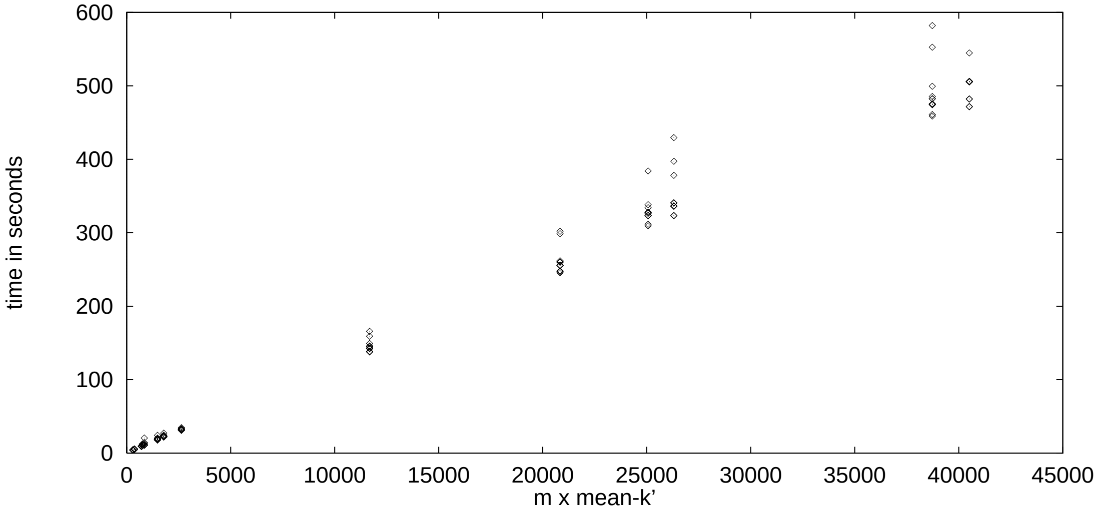

Figure 7: Time to build the molecules shown in Table 1 excluding perturbation time. The horizontal coordinate is size-of-molecule $\times$ mean k'.
Each diamond corresponds to he time to build the surface for one molecule for one particular setting of δ and ϵ as described in Section 6.

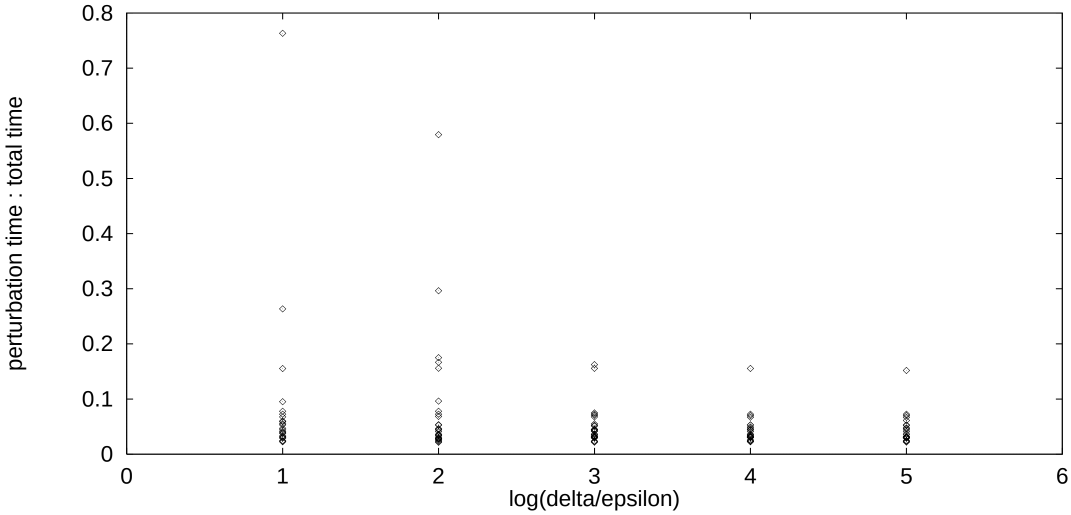

Figure 8: Ratio of perturbation time to total time versus ratio of δ to ϵ.

	1e-3	1e-4	1e-5	1e-6	1e-7	1e-8	1e-9
1e-2	0.993	0.999	0.999	0.999	0.999	1.000	1.000
1e-3		0.999	0.999	0.999	1.000	1.000	1.000
1e-4			0.999	0.999	0.999	0.999	1.000
1e-5				1.000	1.000	1.000	1.000
1e-6					1.000	1.000	1.000
1e-7						1.000	1.000
1e-8							1.000

Table 2: Valid fraction of the δ-sphere for molecule 10 from Table 1. ϵ varies across the table and δ varies downwards.

$1-\cos(\omega)$				
1e-9	1e-10	1e-11	1e-12	1e-13
0.285	0.675	0.890	0.950	0.975

Table 3: Valid fraction of pole positions for molecule 8 from Table 1.

	1e-3	1e-4	1e-5	1e-6	1e-7	1e-8	1e-9
1e-2	0.625	0.937	0.993	0.999	0.999	1.000	1.000
1e-3		0.626	0.937	0.993	0.999	0.999	1.000
1e-4			0.626	0.937	0.993	0.999	0.999
1e-5				0.626	0.937	0.993	0.999
1e-6					0.626	0.937	0.993
1e-7						0.626	0.937
1e-8							0.626

Table 4: Valid fraction of the δ-sphere for the degenerate set of spheres described in Section 6. ϵ varies across the table and δ varies downwards.

time spent on center perturbation can be attributed to a few additional constraints we placed on the poles. In order to simplify certain coding and debugging procedures, we insisted that all spheres share the same pole direction. In addition, the poles were required to be chosen such that no intersection point of a polar arc and a little circle would be within ϵ of any other vertex of the arrangement, and that no polar arc be within ω of the special great circle that is added as part of our "simplified point location" procedure (which we describe in the next section).

We also performed an experiment similar to that of Table 2 for a purposefully degenerate collection of spheres and it is summarized in Table 4. For this set, we arranged 27 spheres in a cube on a unit regular grid. Each sphere had a radius of 1.05 thus producing 2 to 12 degeneracies where 3 little circles intersect at one point on each sphere. In this highly degenerate case, most of the δ-sphere was free even when the ratio of δ to ϵ was as small as 10.

7 Additional Issues in Computing Spherical Arrangements

7.1 Simplified Point Location

We construct the spherical arrangement on each sphere by sequentially adding one sphere at a time to the collection. Each sphere induces a number of little circles on both itself and other spheres. These are added in corresponding pairs. When a new circle is added to a sphere, we must locate in the previously constructed arrangement a point on the little circle. For circles which do not encompass a pole, we choose to locate the polar tangency points. Since polar arcs must be extended from each tangency to the arc segments "above" and "below" the tangency, finding these "upper" and "lower" bounds on the polar arc is sufficient for point location.

In order not to have to search through all of the arcs on a sphere to find the two arcs needed, we use a simple partitioning scheme. Each sphere is divided into sections along the equator. All arcs on the sphere are projected onto the plane of the equator and then outward to the equator. Each section on the equator stores references to the arcs whose projections pass through it. Furthermore, since all little circles are broken at polar tangency points, the equatorial extent of any arc segment can be found by projecting only its endpoints.

Thus, for point location, the point is similarly projected onto the equator and then onto a section. Half of a great circle passing from one pole to the other through the point is constructed and this polar arc is then intersected with the arcs listed in the found section to find the arc immediately "above" and "below" the point. For our implementation, we chose to divide the equator into a fixed number of equal-size sections.

For little circles which surround one of the poles, such a scheme will not work since there are no such tangency points. To ensure simple point location in this case, one great circle passing through the poles is maintained. Thus each little circle without tangencies will intersect this great circle twice. These two points are then used as starting locations for adding the rest of the little circle just as the tangency points would otherwise be used.

Figure 9 shows timings of the code involved in point location during a load of molecule 10 from table 1. The plot is not as conclusive as we might hope (we would like to find a minimum in the graph that corresponds to a good trade-off between query and maintenance time), but it certainly shows an initial negative slope for small numbers of sections and hints at a positive slope for larger values.

7.2 Full vs. Partial Decomposition

To evaluate the experimental advantage of either the partial or full decompositions, we took molecule 4 and timed the algorithm while successively increasing each radius in the radii table used to convert element types to radii. The radii were expanded by a constant each time and the calculations redone. This provided a number of different molecules with different k' values and a somewhat "natural" distribution of spheres in space.

The average value of k' gives a good indication of the complexity of the spherical decompositions constructed since it is the average number of spheres intersecting any given sphere in the arrangement. Thus (average k') $\times m$ is the total number of little circles computed during the construction of the spherical decompositions.

Figures 10, 11, and 12 detail the amount of time spent in each of the phases (decomposition construction, pole perturbation, and center perturbation respectively). The last figure only has one graph since the algorithm for finding centers does not change based on the decomposition method. The timings were stopped at the point where no further increase could be made in the radii due to limited computer time (the algorithms were allowed to run up to six hours). The pole perturbation was found to be the limiting factor.

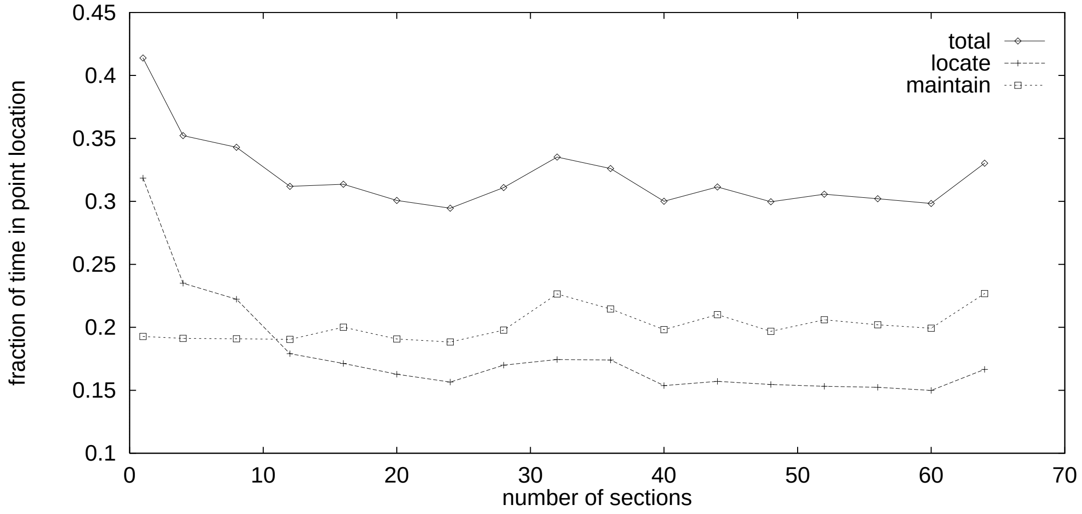

Figure 9: Fraction of the total time of the construction spent in locating points, divided into time spent maintaining the data structure and the time spent querying and locating points on the decomposition.

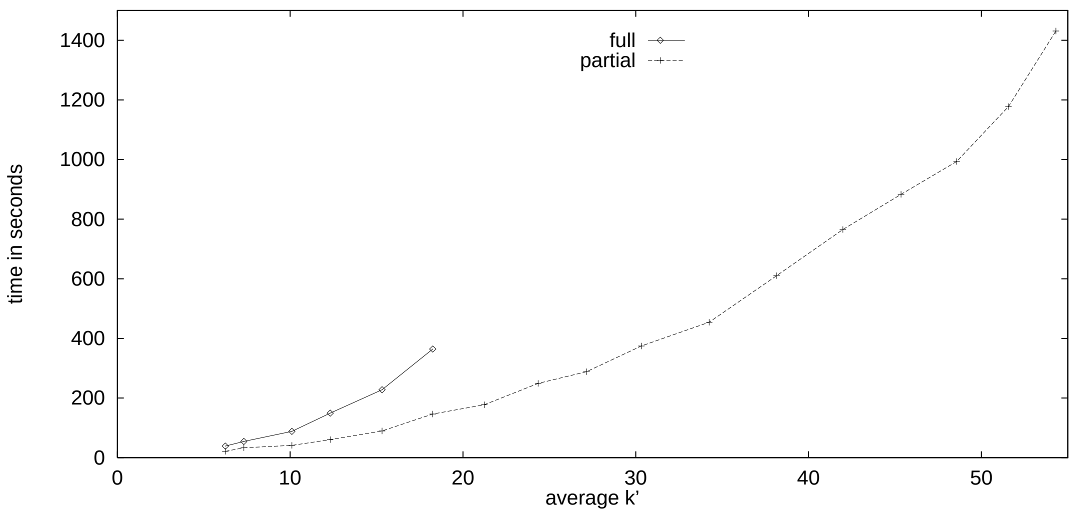

Figure 10: Time spent constructing the decompositions after the perturbation for full and partial decompositions against the mean of k' (the average number of little circles per sphere)

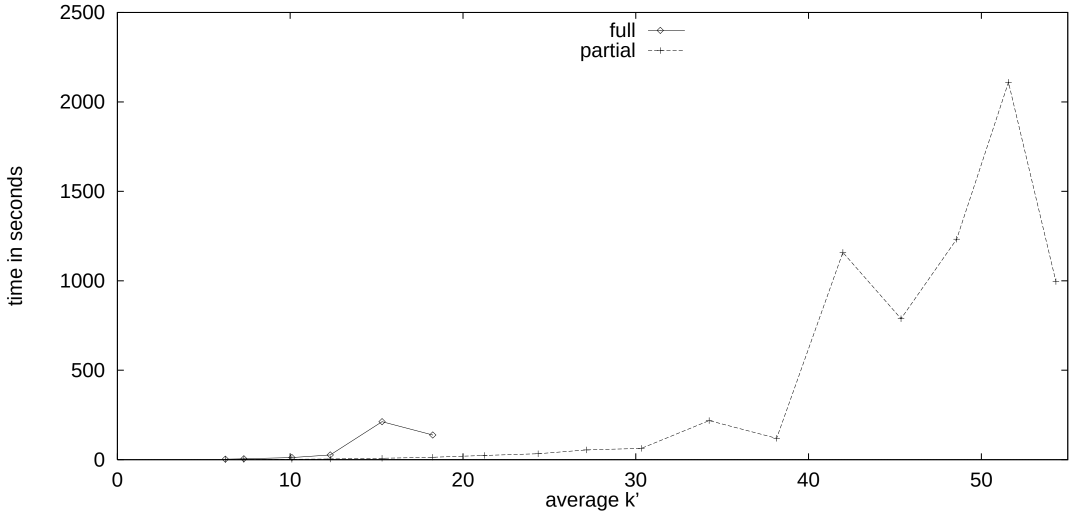

Figure 11: Time spent finding a valid pole direction for full and partial decompositions against the mean of k' (the average number of little circles per sphere)

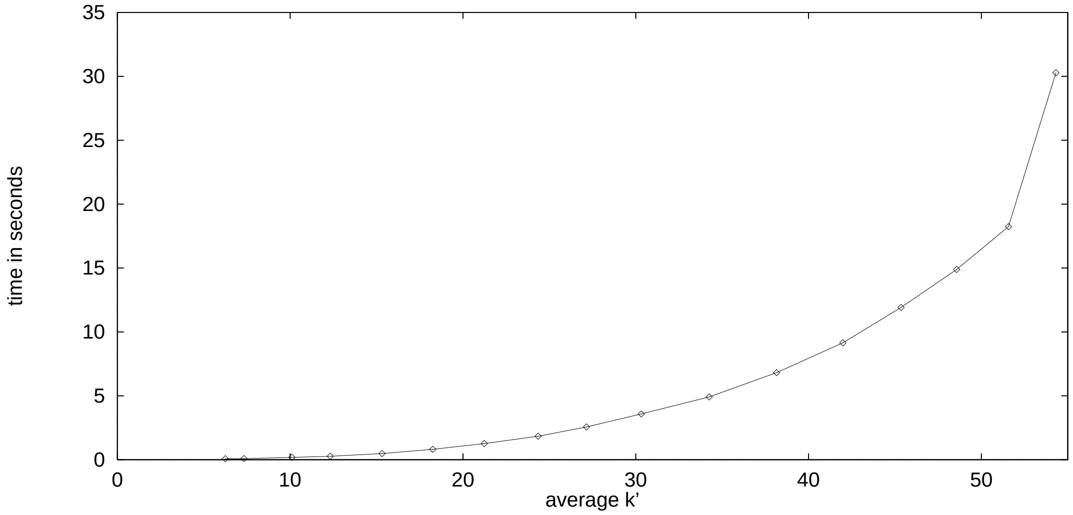

Figure 12: Time spent perturbing the centers of the spheres against the mean of k' (the average number of little circles per sphere)

8 Conclusion

We have presented a perturbation scheme for a collection of spheres in three-dimensional space. Our scheme is suitable for computing with finite precision arithmetic and we have presented experimental results obtained while using standard floating point arithmetic. For a given resolution parameter $\varepsilon > 0$ we perturb the spheres such that features of the three-dimensional arrangement of the spheres (and hence of the two-dimensional spherical arrangement on each sphere) are at least ε apart. Our scheme balances between the size of the perturbation, which we aim to minimize, and the expected running time of the scheme: The smaller the magnitude of the perturbation the longer the expected time it may take to compute a valid perturbation.

The scheme that we have presented is fairly easy to program, it removes degeneracies and in that makes the other parts of the algorithm easier to program, and as the experimental results show it runs efficiently.

Our motivation to develop this scheme is a software package that we have devised aimed to support geometric queries on molecular models. The new scheme has made our algorithms and data structures robust with only little effect on the running and reaction time of the system. We have also presented experimental results showing this small effect. Our software package is currently used by chemists working in rational drug design.

The main direction for further research that we propose is to extend the scheme to other types of arrangements of geometric objects. An obvious limitation of our approach, that may make it unsuitable for certain applications, is that we actually move the input geometric objects from their given placement. However, we believe that there are applications where a small bounded perturbation of the input objects is permissible, since often the precision of the input objects is limited to start with (due to measurement limitations, for example).

Acknowledgment

The molecular modeling package described in the paper has been developed as part of a joint project between the Computer Science Robotics Laboratory at Stanford University and Pfizer Central Research in Sandwich, England. The authors acknowledge the assistance of Jean-Claude Latombe who initiated and supervised the project, Paul Finn of Pfizer Central Research who provided useful guidance, and the help and support of the other participants at Stanford: Lydia Kavraki (now at Rice University), Rajeev Motwani, and Suresh Venkatasubramanian.

References

[1] F. Avnaim, J.-D. Boissonnat, O. Devillers, F. Preparata, and M. Yvinec. Evaluation of a new method to compute signs of determinants. In *Proc. 11th Annu. ACM Sympos. Comput. Geom.*, pages C16–C17, 1995.

[2] L.M. Balbes, S.W. Mascarella, and D.B. Boyd. A perspective of modern methods for computer aided drug design. In *Reviews in Computational Chemistry*, volume 5, pages 265–294. VCH Publishers Inc., 1994.

[3] H. Bronnimann, I. Emiris, V. Pan, and S. Pion. Computing exact geometric predicates using modular arithmetic with single precision. In *Proc. 13th Annu. ACM Sympos. Comput. Geom.*, pages 174–182, 1997.

[4] H. Bronnimann and M. Yvinec. Efficient exact evaluation of signs of determinants. In *Proc. 13th Annu. ACM Sympos. Comput. Geom.*, pages 166–173, 1997.

[5] C. Burnikel, K. Mehlhorn, and S. Schirra. On degeneracy in geometric computations. In *Proc. 5th ACM-SIAM Sympos. Discrete Algorithms*, pages 16–23, 1994.

[6] K. L. Clarkson. Safe and effective determinant evaluation. In *Proc. 33rd Annu. IEEE Sympos. Found. Comput. Sci.*, pages 387–395, 1992.

[7] M.L. Connolly. Analytical molecular surface calculation. *Journal of Applied Crystallography*, 16:548–558, 1983.

[8] M.L. Connolly. Molecular surfaces: A review. *Network Science*, 1996. http://www.awod.com/netsci/Issues/Apr96/feature1.html.

[9] H. Edelsbrunner, M. Facello, P. Fu, and J. Liang. Measuring proteins and voids in proteins. Technical Report HKUST-CS94-19, The Hong Kong University of Science and Technology, 1994.

[10] H. Edelsbrunner and E. P. Mücke. Simulation of simplicity: a technique to cope with degenerate cases in geometric algorithms. *ACM Trans. Graph.*, 9:66–104, 1990.

[11] I. Emiris and J. Canny. An efficient approach to removing geometric degeneracies. In *Proc. 8th Annu. ACM Sympos. Comput. Geom.*, pages 74–82, 1992.

[12] P.W. Finn, D. Halperin, L. Kavraki, J.-C. Latombe, R. Motwani, C. Shelton, and S. Venkatsubramanian. Geometric manipulation of flexible ligands. In Ming C. Lin and Dinesh Manocha, editors, *Applied Computational Geometry: Towards Geometric Engineering*, volume 1148 of *Lecture Notes in Computer Science*, pages 67–78. Springer, 1996.

[13] P.W. Finn, L. Kavraki, J.-C. Latombe, R. Motwani, C. Shelton, S. Venkatsubramanian, and F. Yao. Rapid: randomized pharmacophore identification for drug design. In *Proc. 13th Annu. ACM Sympos. Comput. Geom.*, pages 324–333, 1997.

[14] S. Fortune. Ronustness issues in geometric algorithms. In Ming C. Lin and Dinesh Manocha, editors, *Applied Computational Geometry: Towards Geometric Engineering*, volume 1148 of *Lecture Notes in Computer Science*, pages 9–14. Springer, 1996.

[15] S. Fortune and C. J. Van Wyk. Static analysis yields efficient exact arithmetic for computational geometry. *ACM Trans. on Graphics*, 25(3):223–248, 1996.

[16] M. Goldwasser. An implementation for maintaining arrangements of polygons. In *Proc. 11th Annu. ACM Sympos. Comput. Geom.*, pages C32–C33, 1995.

[17] M.T. Goodrich, L.J. Guibas, J. Hersgberger, and P.J. Tanenbaum. Snap rounding line segments efficiently in two and three dimensions. In *Proc. 13th Annu. ACM Sympos. Comput. Geom.*, pages 284–293, 1997.

[18] D. H. Greene and F. F. Yao. Finite-resolution computational geometry. In *Proc. 27th Annu. IEEE Sympos. Found. Comput. Sci.*, pages 143–152, 1986.

[19] L. J. Guibas and J. Stolfi. Primitives for the manipulation of general subdivisions and the computation of Voronoi diagrams. *ACM Trans. Graph.*, 4:74–123, 1985.

[20] D. Halperin. Arrangements. In Jacob E. Goodman and Joseph O'Rourke, editors, *Handbook of Discrete and Computational Geometry*, chapter 21, pages 389–412. CRC Press LLC, 1997.

[21] D. Halperin and M. H. Overmars. Spheres, molecules, and hidden surface removal. In *Proc. 10th Annu. ACM Sympos. Comput. Geom.*, pages 113–122, 1994.

[22] J. Hobby. Prcatical segment intersection with finite precision output. Technical Report 93/2-27, Bell Laboratories (Lucent Technologies), 1993.

[23] C.M. Hoffmann. *Geometric and Solid Modeling.* Morgan Kaufmann, San Mateo, California, 1989.

[24] C.M. Hoffmann. The problems of accuracy and robustness in geometric computation. *IEEE Computer*, 22(3):31–41, March 1989.

[25] Ming C. Lin and Dinesh Manocha, editors. *Applied Computational Geometry: Towards geometric Engineering.* Springer, 1996.

[26] P.G. Mezey. Molecular surfaces. In K.B. Lipkowitz and D.B. Boyd, editors, *Reviews in Computational Chemistry*, volume 1, pages 265–294. VCH Publishers Inc., 1990.

[27] V. Milenkovic. Verifiable implementations of geometric algorithms using finite precision arithmetic. *Artif. Intell.*, 37:377–401, 1988.

[28] F. P. Preparata and M. I. Shamos. *Computational Geometry: An Introduction*. Springer-Verlag, New York, NY, 1985.

[29] M. F. Sanner, A. J. Olson, and J.-C. Spehner. Fast and robust computation of molecular surfaces. In *Proc. 11th Annu. ACM Sympos. Comput. Geom.*, pages C6–C7, 1995.

[30] R. Seidel. The nature and meaning of perturbations in geometric computing. In *Proc. 11th Sympos. Theoret. Aspects Comput. Sci. (STACS)*, volume 775 of *Lecture Notes in Computer Science*, pages 3–17. Springer-Verlag, 1994.

[31] J. R. Shewchuk. Robust adaptive floating-point geometric predicates. In *Proc. 12th Annu. ACM Sympos. Comput. Geom.*, pages 141–150, 1996.

[32] K. Sugihara. On finite-precision representations of geometric objects. *J. Comput. Syst. Sci.*, 39:236–247, 1989.

[33] K. Sugihara and M. Iri. Two design principles of geometric algorithms in finite-precision arithmetic. *Appl. Math. Lett.*, 2(2):203–206, 1989.

[34] A. Varshney, F.P. Brooks Jr., and W.V. Wright. Computing smooth molecular surfaces. *IEEE Computer Graphics and Applications*, 14:19–25, 1994.

[35] C. K. Yap. A geometric consistency theorem for a symbolic perturbation sch eme. *J. Comput. Syst. Sci.*, 40:2–18, 1990.

[36] C. K. Yap. Robust geometric computation. In Jacob E. Goodman and Joseph O'Rourke, editors, *Handbook of Discrete and Computational Geometry*, chapter 35, pages 653–668. CRC Press LLC, 1997.

[37] C. K. Yap and T. Dubé. The exact computation paradigm. In D.Z. Du and F. Hwang, editors, *Computing in Euclidean Geometry*, pages 452–492. World Scientific, 1995.

Appendix: Shells of Degenerate Placements

In this appendix we give more details on the shape and volume of the shells defining the regions F_2, F_3 and F_4 as mentioned in Section 4; we use the notation established there.

The region $\mathbf{F_2}$ consists of placements of the center of S_{t+1} that induce tangency or near-tangency of S_{t+1} and another sphere. There are two types of tangencies: external and internal. We first describe the shell for external tangency. For a sphere S_i, an exact tangency is induced by placing the center C_{t+1} of S_{t+1} at distance exactly $r_i + r_{t+1}$ away from the center of S_i, namely, $\rho_{i(t+1)} - r_i - r_{t+1} = 0$. We define the potential degeneracy of this type when using floating point with resolution parameter $\varepsilon > 0$ as the union of placements of the center of S_{t+1} such that $-\varepsilon \leq \rho_{i(t+1)} - r_i - r_{t+1} \leq \varepsilon$, which is a spherical shell (i.e., the region sandwiched between two concentric spheres) with center at C_i and radii $r_i + r_{t+1} - \varepsilon$ and $r_i + r_{t+1} + \varepsilon$. Its volume is $\frac{4}{3}\pi[(r_i + r_{t+1} + \varepsilon)^3 - (r_i + r_{t+1} - \varepsilon)^3]$. Similarly the volume of a shell corresponding to internal tangency (assuming $r_{t+1} > r_i$) is $\frac{4}{3}\pi[(r_{t+1} - r_i + \varepsilon)^3 - (r_{t+1} - r_i - \varepsilon)^3]$.

The region $\mathbf{F_3}$ is the union of *toric shells* each defined for a pair of distinct spheres $S_i, S_j \in M_t$. Let C_{ij} denote $S_i \cap S_j$ where both spheres are in their final placement, namely, they have possibly been perturbed. The toric shell for the pair S_i, S_j is the loci of placements of the center of S_{t+1} that will cause S_{t+1} to be tangent, or almost tangent to C_{ij}. Thus it represents the placements of S_{t+1} that may cause two circles on a spherical arrangement to be tangent or almost tangent.

We denote the center of circle C_{ij} by c_{ij} and its radius by r_{ij}. At a point p of tangency between C_{ij} and S_{t+1} there is a plane $\Pi(p)$ that is tangent to S_{t+1}, and such that its intersection with the plane containing C_{ij} is a line $L(p)$ tangent to C_{ij}. If we fix the point p on C_{ij} and hence the line $L(p)$ there is a pencil of planes through $L(p)$ where each plane defines a possible osculation placement of the sphere S_{t+1} and the circle C_{ij} at p. The induced loci of forbidden placements for the center of

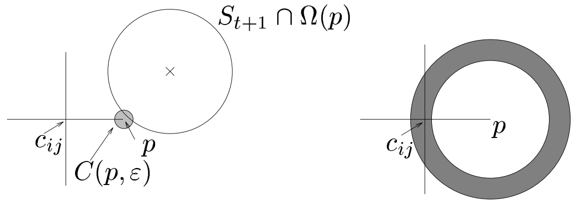

Figure 13: A cross-section of C_{ij} and S_{t+1} on the plane $\Omega(p)$.

S_{t+1} are a circle with center at p, lying on a plane $\Omega(p)$ orthogonal to $L(p)$ and having radius r_{t+1}. We now extend the definition to near-tangency at p and restrict ourselves to the plane $\Omega(p)$.

We assume that the center of S_{t+1} lies on $\Omega(p)$ and hence $S_{t+1} \cap \Omega(p)$ is a great circle of S_{t+1}. We expand a circle $C(p,\varepsilon)$ of radius ε around p. The forbidden placements for the center of S_{t+1} are now all the placement where $S_{t+1} \cap \Omega(p) \cap C(p,\varepsilon) \neq \emptyset$—the shaded annulus in Figure 13.

We repeat this for every point p on C_{ij} and obtain a toric shell. In fact it is only toric-like but for brevity we call it a toric shell. It would have been a real toric shell (the region sandwiched between two tori with the same center, axis of rotation, and major radius) were it not self intersecting as it may possibly be here. To bound the volume of the toric shell, we will first look at the solid of revolution obtained by rotating an external quarter of the annulus around the line through C_{ij} and orthogonal to the plane containing C_{ij}. The obtained volume, which we denote by $V_{1/4}$, is clearly an upper bound on quarter the volume of the toric shell. Let $V_{1/4}(r)$ denote the volume of a quarter torus with major radius r_{ij} and minor radius r. Then $V_{1/4} = V_{1/4}(r_{t+1}+\varepsilon) - V_{1/4}(r_{t+1}-\varepsilon)$.

$$\begin{aligned} V_{1/4}(r) &= 2\pi \int_0^r (u + r_{ij})\sqrt{r^2-u^2}\,du \\ &= 2\pi\Big[\frac{1}{3}(r^2-u^2)^{3/2} + r_{ij}\frac{r^2}{2}\arcsin\frac{u}{r}\Big]\Big|_0^r \\ &= \frac{2}{3}\pi r^3 + \pi^2 r_{ij}\frac{r^2}{2} \end{aligned}$$

It follows that $V_{1/4} = 2\pi^2 r_{ij} r_{t+1}\varepsilon + 4\pi r_{t+1}^2\varepsilon + \frac{4}{3}\pi\varepsilon^3$. Since both r_{ij} and r_{t+1} are bounded by R, we get that the volume of the toric shell is bounded by $4\pi(2\pi+4)R^2\varepsilon + \frac{16}{3}\pi\varepsilon^3$.

The region $\mathbf{F_4}$ is the union of spherical shells each centered at a point of intersection of three distinct spheres in M_t and having radii $r_{t+1}-\varepsilon$ and $r_{t+1}+\varepsilon$. The spherical shell here is the loci of placements of the center of S_{t+1} that will cause S_{t+1} to pass through an intersection point of three distinct spheres in M_t or very close to this intersection point.

Let p denote such an intersection point. The loci of placements of C_{t+1} that will cause S_{t+1} to go through p constitute the sphere centered at p with radius r_{t+1}. It is easily verified that if we wish that p will be ε away from S_{t+1} then the loci of forbidden placements are the spherical shell centered at p with radii $r_{t+1}-\varepsilon$ an $r_{t+1}+\varepsilon$. Its volume is $\frac{4}{3}\pi[(r_{t+1}+\varepsilon)^3 - (r_{t+1}-\varepsilon)^3]$.

Bounding the volume of $\mathbf{F_2}$, $\mathbf{F_3}$, and $\mathbf{F_4}$. Let M be a collection of spheres as defined in Theorem 2.1. Also, as above, let $R := \max_{i=1}^n r_i$, and let k denote the maximum number of spheres of M intersecting a single sphere of M. Given a parameter $\varepsilon > 0$, we wish to determine the parameter $\delta = f(k,\varepsilon,R)$ such that the volume of the forbidden region inside $B(C_{t+1},\delta)$ is less than half the volume of $B(C_{t+1},\delta)$. Let $VB := \text{Volume}(B(C_{t+1},\delta))$, and let $VF := \text{Volume}(F_2 \cup F_3 \cup F_4)$.

Note that there are at most k external spherical shells defining the region F_2 and at most k internal shells, at most $\binom{k}{2}$ toric shells defining the region F_3, and at most $2\binom{k}{3}$ spherical shells defining the region F_4. Therefore we obtain the following bounds on the volume of these regions:

$$\begin{aligned}\text{Volume}(F_2) &\leq k\frac{4}{3}\pi[(2R+\varepsilon)^3-(2R-\varepsilon)^3]+k\frac{4}{3}\pi[(R+\varepsilon)^3-(R-\varepsilon)^3] \\ &\leq \frac{4}{3}\pi k(30R^2\varepsilon+4\varepsilon^3)\end{aligned}$$

$$\text{Volume}(F_3) \leq \binom{k}{2}[4\pi(2\pi+4)R^2\varepsilon+\frac{16}{3}\varepsilon^3] \leq \frac{1}{2}k^2[4\pi(2\pi+4)R^2\varepsilon+\frac{16}{3}\pi\varepsilon^3]$$

$$\text{Volume}(F_4) \leq 2\binom{k}{3}\frac{4}{3}\pi[(R+\varepsilon)^3-(R-\varepsilon)^3] \leq 2\binom{k}{3}\frac{4}{3}\pi(6R^2\varepsilon+2\varepsilon^3) \leq \frac{4}{9}k^3\pi(6R^2\varepsilon+2\varepsilon^3)$$

$$\begin{aligned}VF &\leq \pi R^2\varepsilon[40k+(4\pi+8)k^2+\frac{8}{3}k^3]+\varepsilon^3[\ldots] \\ &\leq 5.13\pi R^2\varepsilon k^3 \text{ (assuming } k\geq 10 \text{ and } \varepsilon \ll k,R) .\end{aligned}$$

Finally, we choose δ such that $VB=\frac{4}{3}\pi\delta^3>2VF$. Thus we let $\delta := 2k\varepsilon^{1/3}R^{2/3}$.